5D quantum dynamics of the H2@SWNT system: Quantitative study of the rotational-translational coupling

M. Mondelo-Martell and F. Huarte-Larrañaga

Citation: The Journal of Chemical Physics **142**, 084304 (2015); doi: 10.1063/1.4913293
View online: http://dx.doi.org/10.1063/1.4913293
View Table of Contents: http://scitation.aip.org/content/aip/journal/jcp/142/8?ver=pdfcov
Published by the AIP Publishing

5D quantum dynamics of the H_2@SWNT system: Quantitative study of the rotational-translational coupling

M. Mondelo-Martell and F. Huarte-Larrañaga[a)]
Departament de Química Física & Institut de Química Teòrica i Computacional (IQTCUB), Universitat de Barcelona, C/ Martí i Franqués 1, 08028 Barcelona, Spain

(Received 13 November 2014; accepted 10 February 2015; published online 25 February 2015)

The dynamics of the dihydrogen molecule when confined in carbon nanotubes with different chiralities and diameters are studied by using a 5 dimensional model considering the most relevant degrees of freedom of the system. The nuclear eigenstates are calculated for an (8,0) and a (5,0) carbon nanotubes by the State-Average Multiconfigurational Time-dependent Hartree, and then studied using qualitative tools (mapping of the total wave functions onto given subspaces) and more rigorous analysis (different kinds of overlaps with reference functions). The qualitative analysis is seen to fail due to a strong coupling between the internal and translational degrees of freedom. Using more accurate tools allows us to gain a deeper insight into the behaviour of confined species. © *2015 AIP Publishing LLC.* [http://dx.doi.org/10.1063/1.4913293]

I. INTRODUCTION

The study of the confinement of gaseous species inside nanostructured materials (*quantum confinement*) has become a matter of study in the last years, both theoretically and experimentally.[1–3] This interest arises due to the unique phenomena that take place when a molecule is embedded in cavities within the nanometric scale, which may be seen as quasi-zero or quasi-one-dimensional spaces. Among these effects, we find distortions of the electronic structure and geometry of the species,[4] as well as changes in their dynamic behavior due to a strong translation-rotation coupling.[5–8] These effects lead to potential applications in chemistry and physics: they allow a tight control of certain reactions,[9] or the separation of isotopes of gaseous species at the molecular level, known as *quantum sieving*.[3,10] In particular, the hydrogen molecule (H_2) has been a popular target for these studies due to the interest of nanostructures as hydrogen storage devices for technological applications. Back in 1999, FitzGerald *et al.*[11] studied the neutron scattering spectra of the hydrogen molecule confined in the octahedral and tetrahedral interstitial sites of a C_{60} lattice both theoretically and experimentally, in one of the first works on the dynamics of a confined molecule considering both rotation and translation. Later on, attention was shifted to other carbon allotropes, such as carbon nanotubes (CNTs). For this kind of system, Yildirim *et al.* made an extensive formal study of the energetic levels of hydrogen using a cylindrical-symmetry potential energy surface model.[6,12] Later on, Gray and coworkers improved the potential model and were able to give deeper insight into the system with a four dimensional Hamiltonian which did not take into account the vibrational degree of freedom (DoF).[5] The first five-dimensional study of hydrogen confined in carbon nanotubes, considering hydrogen's vibration, was later carried out by some of us.[13] This research field has been greatly benefited lately by the valuable contributions of Bačić and coworkers, who have made rigorous calculations of the hydrogen molecule in metal-organic frameworks (MOFs),[7] of hydrogen endofullerenes,[2] and of the HD molecule confined in a clathrate hydrate structure.[1]

In the absence of a confining potential, the internal (rotation and vibration) and translational degrees of freedom of a given molecule would be perfectly separable. This means that the total wave function could be described as the direct product of a free particle and an internal motion function, with quantum numbers l, m (rotation), and v (vibration),

$$\Phi^v(\vec{x},\theta,\phi) = e^{ik\vec{x}}\psi_l^{vm}(\rho,\theta,\phi). \tag{1}$$

When confinement appears, the potential does not only affect the translational degree of freedom, which is now quantized as it corresponds to a bound system, but also couples the internal degrees of freedom and the translation of the molecule. Due to this coupling term, the wave functions describing the final system will not be a direct product of the functions for the individual degrees of freedom, but rather a mixture of them

$$\Phi^v(\vec{x},\theta,\phi) = \sum_{n_x=0}^{\infty}\sum_{n_y=0}^{\infty}\sum_{l=0}^{\infty}\sum_{m=-l}^{l} c_{n_x,n_y,l,m} H_{n_x n_y}(\vec{x}) \times Y_l^m(\theta,\phi), \tag{2}$$

and therefore the internal and translational quantum numbers cannot be considered good quantum numbers.

It is commonly accepted that very light molecules, such as H_2 and D_2, represent an exception to the previous statement. This is so because these species present an exceptionally large moment of inertia that causes the separation between energy levels in the unconfined problem to be very large. Therefore, the mixing of states with different l values due to the coupling with the translational degree of freedom in a confined case is small enough to consider l as a good quantum number. This is the idea followed by Yildirim *et al.* for their formal analysis of the confinement of molecular hydrogen in different

a)Electronic mail: fermin.huarte@ub.edu

nanostructures.[6] However, Gray *et al.* gave the first hints on the fact that this assumption does not hold for the tightest confining potentials, such as the one generated by a (8,0) Single-Walled Carbon Nanotube (SWCNT).[5]

In the present work, we want to go one step further from the previous studies of nanoconfined species by performing a rigorous quantitative study of the quantum eigenstates of a hydrogen molecule inside single-walled carbon nanotubes of different chiralities: (8,0), which accounts for the narrowest nanotube in which physisorption of hydrogen is energetically favourable, and (5,0), which will serve as example of an extremely tight confining potential. The full dimensional eigenstates of the nanoconfined molecule will be interpreted in terms of the eigenfunctions of a separable H_2@SWCNT model.

This paper is organized as follows: first, the model used to describe the physical system and the potential energy surface is discussed. In Sec. III, the approach used to compute the eigenstates of the system is explained. Also, details are given of the multiconfigurational time-dependent Hartree method (MCTDH), which is used to carry out the quantum dynamics calculations. Section IV is devoted to the analysis of the eigenstates themselves and is divided into Subsections IV A and IV B. In Sec. IV A, we focus in the qualitative description, based on the graphical inspection of two dimensional projections of the total wave function in different subspaces (namely, the translational subspace, which takes into account the x and y coordinates, and the rotational subspace in which we find θ and ϕ). Subsection IV B presents a quantitative approach that allows a rigorous description of the wave function based on its overlap with a set of known basis functions. Section V summarizes our results.

II. DESCRIPTION OF THE SYSTEM

Our model consists of a single hydrogen molecule embedded in the hollow cavity of a SWCNT with either (8,0) or (5,0) chirality, hereafter referred to as H_2@(8,0) and H_2@(5,0), respectively. Both nanotubes are represented by concatenating 20 unit cells in order to mimic an infinitely long nanotube, thus making edge effects disregardable. The geometry of the corresponding unit cells has been obtained from a CRYSTAL09[14,15] optimization using the B3LYP functional and a 6-21G basis set. These optimizations yield a nanotube diameter of 7.0 bohrs for the (5,0) CNT and 12.1 bohrs for the (8,0), with an internuclear C-C distance of ~4.5 bohrs.

Regarding the confined molecule, five degrees of freedom (DoFs) are considered, as it can be seen in Figure 1: translation of the center of mass of the molecule in the xy plane, full rotation (θ, ϕ), and vibration (ρ). Note that we do not account for the translation along the nanotube's axis (z). This is justified in terms of the length of the nanotube. Moreover, in case of the (8,0) nanotube, the corrugation of the potential along this direction is small enough not to expect changes of the overall results due to the fixing of the coordinate in a given arbitrary point of the z dimension. This corrugation is much more important in case of the (5,0) nanotube, and the study is carried out fixing the z coordinate of the c.o.m. at exactly the minimum of the Potential Energy Surface (PES) corresponding to center of the unit cell of the system.

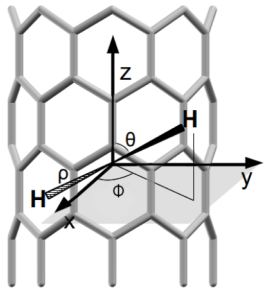

FIG. 1. Scheme of the degrees of freedom considered for the H_2 molecule in the present work.

The full Hamiltonian for this system, H_{5D}, is therefore given by

$$\hat{H}_{5D} = -\frac{\hbar^2}{2\mu_{H_2}}\left(\frac{\partial^2}{\partial\rho^2} + \frac{2}{\rho}\frac{\partial}{\partial\rho} + \frac{1}{\rho^2}\frac{\partial^2}{\partial\theta^2} + \frac{1}{\rho^2}\frac{1}{\sin^2\theta}\frac{\partial^2}{\partial\phi^2}\right) - \frac{\hbar^2}{2m_{H_2}}\left(\frac{\partial^2}{\partial x^2} + \frac{\partial^2}{\partial y^2}\right) + \hat{V}(\rho,\theta,\phi,x,y). \quad (3)$$

To model the five dimensional potential energy operator, we used the same 5D potential energy function used by Suárez and Huarte-Larrañaga.[13] This is a semiempirical potential which accounts for two separable terms: the H–H interaction, V_{H-H} and the van der Waals interactions between the hydrogen atoms and *each* of the carbon atoms in the nanotube, V_{C-H}. The covalent interaction is modelled by a Morse potential,[16] using the parameters D_e = 0.1746 hartree, a = 1.0271 bohr^{-1}, and R_e = 1.4 bohrs. The weak dispersion forces are approximated using the Novaco and Wroblewski potential[17] previously used by Gray:[5] a pair-interaction Lennard-Jones potential with parameters ϵ = 2.82 Å and σ = 0.0605 kcal/mol,

$$\hat{V}_{5D} = V_{H-H}(\rho) + V_{C-H}(\rho,\theta,\phi,x,y), \quad (4)$$

$$\hat{V}_{C-H}(\rho,\theta,\phi,x,y) = \sum_{i=1}^{2}\sum_{j=1}^{Nc} V_{i,j}^{LJ}(d_{H_i-C_j}). \quad (5)$$

It is worthwhile mentioning at this point that there has been some controversy concerning the values of the Lennard-Jones parameters to be used in this kind of systems. However, given that the aim of our work is providing a systematic scheme to characterize the eigenstates of the confined molecule rather than predicting accurate energy splittings, we restrain ourselves to the Lennard-Jones values we have used in the recent past.

Relevant qualitative information about H_2@(8,0) and H_2@(5,0) systems can be extracted just from the shape of their respective PES's. Comparing some features of the potential with experimental results tells us about the suitability of the overall function, and it helps to understand the results of the simulations in the different degrees of freedom. Therefore, a brief discussion of the potential energy surface is given next.

Figure 2 shows a cut of the relaxed PES along the ρ coordinate for the free hydrogen molecule and both the H_2@(8,0) and H_2@(5,0). This representation allows us to find the equilibrium internuclear distance of the molecule in different conditions, as

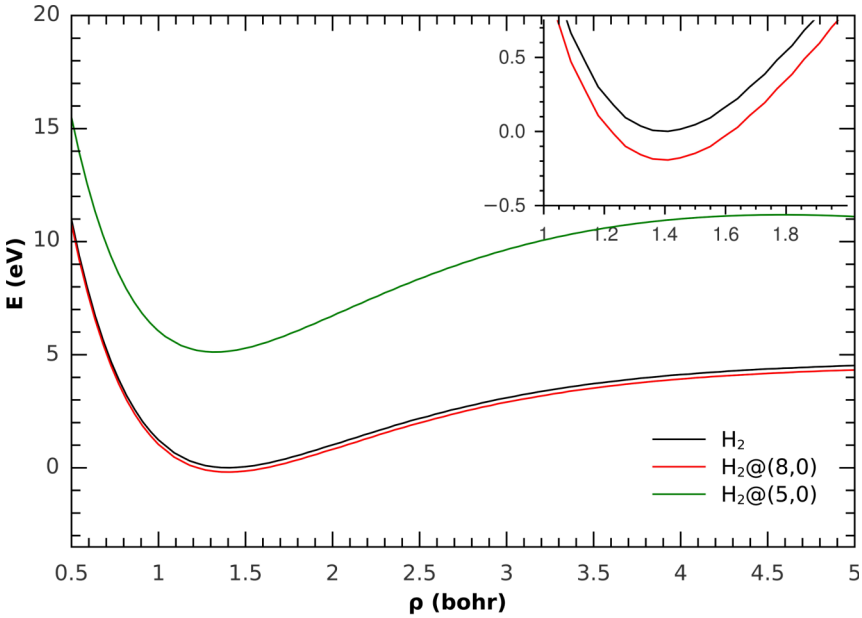

FIG. 2. Potential cut along the ρ coordinate for three different systems: a free hydrogen molecule, a hydrogen molecule embedded in a (8,0) carbon nanotube, and the same molecule in a (5,0) nanotube. Inset: detail of the energy difference between the free molecule and the H_2@(8,0) system. Energy values are referred to the energy of the free H_2 molecule at equilibrium distance.

well as a first approximation to the adsorption energy. Concerning the equilibrium distance, it is seen that there is not a significant change with respect to the free molecule (1.41 bohrs) when the molecule is confined in a (8,0) nanotube. Instead, this distance is slightly decreased to 1.3 bohrs when the nanotube has a (5,0) chirality. This is related to the small diameter and size of the unit cell of this last nanotube: the hydrogen molecule feels a strong repulsion from the C atoms in the cage and tends to shorten the bond to minimize this repulsion. This is related to the second feature that can be extracted from this particular potential cut: the system's minimum energy is slightly lower for the molecule trapped in a (8,0) nanotube than that of the free H_2, which indicates that the absorption is energetically favourable. On the other hand, this minimum is much higher for the (5,0) nanotube, which means that now adsorption is not energetically favourable. This is consistent with some molecular dynamics calculations which show that these nanotubes are way too narrow for hydrogen to be physisorbed in their endohedral sites.[18] The H_2@(5,0) system is therefore not a realistic one, but nevertheless will be useful to illustrate extreme confinement situations. Concerning the translational degrees of freedom, the 2D relaxed energy plots show that both nanotubes create an anharmonic potential with an absolute minimum in the center of the structure. As it can be seen in Figure 3, the potential created by the (5,0) structure is much tighter than the one of the (8,0) CNT due to the smaller diameter. Hence, the wave functions of the former system are expected to be much more distorted than the ones obtained for the latter.

Finally, the cut of the PES along the rotational (θ, ϕ) coordinates gives us another feature of the system: the hindrance that the potential imposes to the rotation of the H_2 molecule (see Figures SF1 and SF2 in the supplementary material[19] for the plots of these projections). For the wider (8,0) nanotube, this rotation occurs through a quite low barrier (20 meV), and the profile in the ϕ dimension is constant even for the perpendicular orientation of the diatom ($\theta = 2/\pi$). This may lead to thinking that the rotational functions will be very similar to the ones of a free rotator. Instead, the rotational barrier for the H_2 molecule in the (5,0) carbon nanotube is exceptionally higher (3.41 eV). This energy is too high for the molecule to overcome, and therefore rotation along the θ dimension would not be possible inside this nanotube. Due to the symmetry of the system and this high barrier, we end up with a symmetric double-well potential, and the functions are expected to be only loosely related to spherical harmonics.

III. CALCULATION OF THE NUCLEAR EIGENSTATES

The eigenstates of the studied system were calculated following the State Average Multiconfigurational Time-dependent Hartree (SA-MCTDH) scheme developed by Manthe.[20] It is based on the iterative application of the operator to be diagonalised onto a set of wave functions. In the case of energy eigenstates, one can apply the Boltzmann operator, $e^{-\beta\hat{H}}$ instead of the Hamiltonian operator, which is equivalent to the propagation of the set of wavepackets in imaginary time, β.

A. State-average multiconfigurational time-dependent Hartree approach

The MCTDH approach is an efficient algorithm to propagate high-dimensional wavepackets.[21] In this method, an f-dimensional system is described by p logical coordinates Q_k, such that $p \leq f$. Then, an ansatz is constructed as linear combination of Hartree products, each one of these being a direct product of time-dependent functions corresponding to the different logical coordinates, the so called Single Particle Functions (SPFs). Hence, the expression for the ansatz is

$$\Psi(Q_1,\ldots,Q_p,t) = \sum_{j_1=1}^{n_1}\cdots\sum_{j_p=1}^{n_p} A_{j_1\cdots j_p}(t)\prod_{k=1}^{p}\varphi_{j_k}^{(k)}(Q_k,t), \quad (6)$$

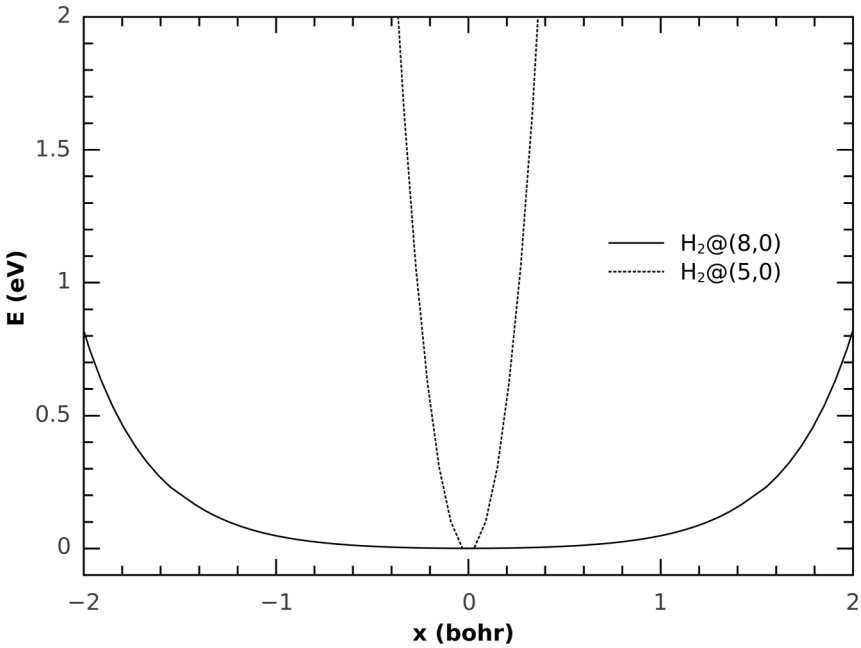

FIG. 3. Cut of the relaxed 5D potential energy surface along the x coordinate for both the (8,0) and the (5,0) nanotubes. The energy origin has been shifted to 0 in both cases.

where the SPFs are denoted by $\varphi_{j_k}^{(k)}(Q_k,t)$ and k runs over all coordinates of the system. $A_{j_1\cdots j_p}(t)$ represent the coefficients of the different Hartree products of the linear combination, and a sum runs for each coordinate in the system depending on the number of SPFs used to describe each coordinate k, j_k.

The SPFs are in turn represented in a *primitive* time-independent basis set, which is in general based on a Discrete Variable Representation (DVR) or FFT grid

$$\varphi_j^{(k)}(Q_k) = \sum_{l=1}^{N_k} a_{l_j}^{(k)} \chi_l^{(k)}(Q_k). \tag{7}$$

Applying the Dirac-Frenkel variational principle to this ansatz, two sets of coupled equations of motion are derived: one set for the $A_{j_1\cdots j_p}(t)$ coefficients and another one for the SPFs. The *double layer* representation is the reason why the MCTDH scheme has a such great efficiency compared to the *standard wavepacket* approach, in which the total wave function is represented completely in a time-independent basis: since the SPFs are time-dependent, they adapt to the total wave function at each time step, and therefore, a relatively small number of them are needed for a good description of the system. This decreases the numerical effort required to integrate the equations of motion for the ansatz, while retaining much of the accuracy. For further detail, the reader is referred to the monograph edited by Meyer *et al.*[22]

As mentioned before, the SA-MCTDH approach has been used in the present work to obtain the eigenenergies and eigenstates of the system under study, through diagonalization of the Boltzmann operator on a basis formed by a set of orthonormal wavepackets propagated in imaginary time. This set of wavepackets is represented in a common basis of SPFs, which allows an easy orthogonalization of the set after each propagation. However, it also carries implicitly an important drawback: since the best basis set to represent the average wave function will not be necessarily the optimal set for each individual state, one may need more basis functions to converge the results than if an individual wavepacket was propagated for each state. Nevertheless, as it is shown elsewhere,[20] it is a powerful approach to calculate nuclear eigenstates.

One last remark must be made about the MCTDH scheme: its maximum efficiency is reached when the whole Hamiltonian is expressed in a product-like form, since then the integration of the equations of motion is much more straightforward. This can be easily achieved for the kinetic energy operator,[23] but not for the potential energy operator in its general form. The *Correlation Discrete Variable Representation* (CDVR) scheme developed by Manthe[24] allows using a general potential energy surface in a MCTDH calculation while largely retaining the accuracy, and this approach was used in our program to implement the potential function as shown in Eq. (5).

B. Numerical details

As it was outlined previously, the MCTDH approach is based on a two layer representation of the full-dimensional wave function. In our case, the wave function is expanded onto a configuration space obtained from the direct product of five sets of SPFs, one for each DoF of the system. Then, each of these SPFs is represented in a suitable time-independent basis. Four of the SPFs sets used in the present work (ρ, ϕ, x and y) are represented in a Fourier method grid. However, a particular issue appears when representing the orientation of the H_2, θ: due to the $\frac{1}{\sin^2\theta}$ term that appears in Eq. (3), a singularity arises in the Hamiltonian for $\theta = 0$, i.e., if the H_2 molecule is oriented parallel to the nanotube's axis. This singularity becomes specially important in the present case, due to the strong alignment of the confined molecule along the nanotube axis (z), $\theta = 0$. For this reason, the θ degree of freedom was represented in a cot-DVR scheme specially designed to avoid this singularity.[25]

The size of the primitive basis set itself, as well as the number of SPFs needed to represent each DoF, depends on the potential to which the hydrogen molecule is exposed. Hence, for the (8,0) nanotube, the number of SPFs for each degree

TABLE I. Numerical details of the basis set used for the calculations of the H_2@(8,0) system. Magnitudes given in bohrs or radians, correspondingly.

Degree of freedom	Number of SPFs	Lower limit	Upper limit	Number of functions	Initial position
ρ	2	0.5	5.0	32	1.41
θ	7	0.0	π	64	$\pi/2$
ϕ	7	0.0	2π	64	0.0
x	5	−3.5	3.5	32	0.0
y	5	−3.5	3.5	32	0.0

of freedom was increased until the numerical convergence of more than 40 excited states was achieved. The detailed information about the parameters used for the representation of the wave function is given in Table I.

Due to the extreme tightness of the potential generated by narrower nanotubes, this basis had to be changed significantly in the case of the H_2@(5,0) system: first of all, the range of the x and y coordinates was reduced to go just from −0.8 to 0.8 bohrs, since for larger distances from the nanotube's center, the potential was way too repulsive (see Figure 3). Then, once this range was set, the number of SPFs was adjusted to achieve the numerical convergence of up to 26 eigenstates. The converged parameters for the wave function representation are shown in Table II. Note that the number of SPFs needed to converge the calculation increases in the vibrational degree of freedom. This seems to indicate that the coupling between the internal and translational DoFs will be much more important for this system than for the previous one.

With these basis sets, the eigenstates for the H_2@(8,0) and H_2@(5,0) were computed following the SA-MCTDH approach explained above. A value of β = 525 a.u. was used in both systems for the Boltzmann operator.

In the case of the (8,0) nanotube, the 50 lower energy eigenstates were converged after 27 iterations. Energy values are listed in the second column of Table III. Two main features stand out in the energy spectrum. The first is its high zero point energy of 2580 cm^{-1}, which is 421 cm^{-1} larger than that of the free H_2. This feature was already pointed out in a previous work by some of us,[13] where it was argued that this increase of the Zero Point Energy (ZPE) appears not only because of the quantization of the translational degree of freedom, but it is also an evidence of the coupling between the different degrees of freedom. The second feature to highlight is that the eigenstate spectrum is radically densified under confinement conditions. The reason for this increase in the density of eigenenergies is threefold: first of all, the confining potential quantizes the translational motion of H_2. Second, the cylindrical symmetry of the potential breaks the degeneracy of rotational eigenstates. And finally, mixed states are expected to appear in the spectrum due to the coupling between the internal and translational degrees of freedom.

TABLE II. Numerical details of the basis set used for the calculations of the H_2@(5,0) system. Magnitudes given in bohrs or radians, correspondingly.

Degree of freedom	Number of SPFs	Lower limit	Upper limit	Number of functions	Initial position
ρ	4	0.5	5.0	32	1.45
θ	8	0.0	π	64	$\pi/2$
ϕ	6	0.0	2π	64	0.0
x	4	−0.8	0.8	32	0.0
y	4	−0.8	0.8	32	0.0

TABLE III. Relevant results of the qualitative assignation of the calculated eigenstates of the H_2@(8,0) system. Energies are given in wavenumber units related to the ground state energy of 2580 cm^{-1}. See text for the meaning of the h label.

State	ΔE	n_x	n_y	l	|m|	k
0	0	0	0	0	0	0
1	59	0	0	1	0	0
2	171	0	0	1	1	0
3	171	0	0	1	1	0
4	265	1	0	0	0	0
5	265	0	1	0	0	0
6	310	1	0	1	0	0
7	310	0	1	1	0	0
8	343	0	0	2	0	0
9	346	0	0	2	1	0
10	346	0	0	2	1	0
11	428	h	h	2	2	0
12	429	0	0	2	2	0
13	429	0	0	1	1	0
14	462	h	h	2	2	0
15	462	h	h	2	2	0
16	503	h	h	2	2	0
17	550	(1,0)/(0,1)		0	0	0
18	550	(1,0)/(0,1)		0	0	0
19	572	(2,0)/(0,2)		0	0	0
20	580	(1,0)/(0,1)		1	0	0
21	580	(1,0)/(0,1)		1	0	0
22	590	h	h	2	1	0
23	597	(2,0)/(0,2)		1	0	0
24	615	1	0	0	0	0
25	615	0	1	0	0	0

Regarding the extremely confining (5,0) nanotube, 26 eigenstates were converged after 20 iterations. The corresponding eigenenergies are reported in Table IV. In this case, the ZPE for the system is outstandingly high (9273 cm^{-1}). An important part of this ZPE (4278 cm^{-1}) is due to the quantization of the translational degree of freedom, and its high value is consistent with the extreme tightness of the potential created by such a narrow nanotube. The remaining 4995 cm^{-1} comes from the combined effect of the vibrational and rotational ZPE (this latter is no longer 0, due to the hindrance to rotation) plus the energy due to the coupling between the degrees of freedom.

IV. EIGENSTATE ANALYSIS

In this section, we present our analysis of the eigenstates of the confined hydrogen system employing two schemes, one based on the graphical inspection of the nodal structure of the wave function and a more rigorous analysis consisting in the study of the overlap of the system's eigenfunctions with models of reduced dimensionality. The strengths and weaknesses of each approach will be discussed next.

TABLE IV. Results of the qualitative assignation of the different degrees of freedom for the H_2@(5,0) system. Energies are relative to the ground state energy of 9273 cm^{-1}.

State	ΔE	n_x	n_y	l	|m|	k
0	0	0	0	1	0	0
1	0	0	0	1	0	0
2	3552	0	0	1	1	0
3	3552	0	0	1	1	0
4	3552	0	0	1	1	0
5	3552	0	0	1	1	0
6	3591	0	1	1	0	0
7	3591	0	1	1	0	0
8	3591	1	0	1	0	0
9	3591	1	0	1	0	0
10	4636	0	0	1	0	1
11	4636	0	0	1	0	1
12	6674	0	0	1	3	0
13	6674	0	0	1	3	0

A. Low-coupling limit: Assignment based on the nodal pattern

The first attempt in the description of the eigenstates of our system was to carry out a qualitative analysis of the wave functions. As it was discussed in Sec. I, for a fully separable Hamiltonian, the total wave function would be described as a product of individual wave functions, each being the solution for each degree of freedom in the Hamiltonian. If the Hamiltonian is not separable but the coupling between the internal and translational DoFs is small (*low-coupling limit*), one can still write the total wave function approximately as a direct product of a translational and a rovibrational wave function. Our approach is based on the mapping of the total 5-D function into subspaces corresponding to the translational (x and y), rotational (θ and ϕ), and vibrational (ρ) degrees of freedom, thus allowing a graphical representation of the reduced probability density in these subspaces. Then, these mappings can be directly compared with the solutions for a hypothetical separable system, which corresponds to direct products of a two-dimensional harmonic oscillator function ($H_{n_x,n_y}(x,y)$) accounting for the translational DoFs, a spherical harmonic ($Y_l^m(\theta,\phi)$) accounting for the rotation, and a Morse function ($M_k(\rho)$) to include vibration. Comparing the nodal pattern of the mapped probability densities with the different states of the separable problem, one tries to obtain a one-to-one correspondence between the confined and the free systems, and assigns a quantum number to each degree of freedom for a given state: n_x and n_y for the translation, l and |m| for the angular momentum, and k for the vibration. The quantity |m| is used instead of simply m because of the cylindrical symmetry of the system, which will force the degeneracy of the energy of states with equal l and |m|.

Some relevant results of the qualitative analysis for hydrogen confined in the wider nanotube are found in Table III. As it is seen in this table, no excitation is found in the vibrational degree of freedom, and therefore, the selection of the rigid rotor functions to study the internal degrees of freedom of the H_2 molecule seems justified for low energy eigenstates.

This graphical inspection was enough to relate most of the eigenstates of the system to a given pair of rotational and translational reference functions and assign the corresponding quantum numbers. The procedure is illustrated in Figure 4 for the first excited state. In the figure, the projection of the total wave function onto the rotational and translational subspaces is shown. For the translational projection, the absolute square value of the function is shown in the xy plane, while for the rotational subspace, the function is given in spherical coordinates. In this representation, the radius of the plot is related to the squared absolute value of the function for a given pair of θ and ϕ angles. The plane corresponding to a value of $\theta = \pi/2$, that is for the perpendicular orientation of the internuclear axis with respect to the carbon nanotube, is also given to ease the interpretation. One can observe that, in this state, this plane is precisely a nodal plane in the θ coordinate. This nodal plane in the θ dimension, together with the presence of no nodes in the ϕ degree of freedom, corresponds to a Y_1^0 spherical harmonic, so we assign the quantum numbers $l = 1$, $m = 0$ to the first excited state. Since there are no nodal planes in the xy plane of the translational subspace mapping, we also assign the quantum numbers $n_x = 0$ and $n_y = 0$. Finally, for the internuclear distance subspace, again no nodes are found and therefore the state is labeled as $k = 0$. However, although the study of the nodal pattern enables a one-to-one correspondence between most of the H_2@(8,0) states and the free H_2 ones, a deeper study of Table III shows that this assignation is not consistent in all cases. This is evidenced by the fact that some of the states yield exactly the same quantum numbers under the nodal planes' criterion, even though they are clearly different functions with different energies. This is the case of the set formed by the 2nd, 3rd (degenerate), and 13th excited states, for instance. Oppositely, the 12th and 13th excited states are energetically degenerate despite the fact that the analysis of nodal planes tells us that they should have different values of |m|. A closer look to the functions shows us why this method is not good enough to establish a clear correspondence between the confined and free H_2 states. For instance, the ground state wave function mapped on the orientational subspace (θ, ϕ), shown in Figure 5, shows no nodal plane in this projection. In our qualitative approach, this means that this function corresponds to a $l = 0$, $m = 0$ state. However, a significant depression is found for values of the polar angle θ near to $\pi/2$, which indicates that there is a significant mixing of rigid rotor states in order to give rise to this function. A similar case is found in the translational mapping of the 11th, 14th, 15th, 16th, and 22nd excited states. These projections, shown in Figure 6 for the 11th excited state, present a minimum of probability in the $x = 0$, $y = 0$ point, which cannot be strictly considered a nodal point. This structure does not correspond to any eigenstate of an anharmonic oscillator, and therefore, an h state is used to label the n_x and n_y quantum numbers. Finally, a more subtle example is found in the translational projection of the remaining eigenstates: there are slight differences in the overall shape for many of the functions without any nodal plane that may be therefore labelled as $H_{0,0}$. These variations imply that again there is a significant coupling between rotation and translation.

As expected, the inaccuracies of the qualitative inspection method are even more noticeable in case of the narrower (5,0)

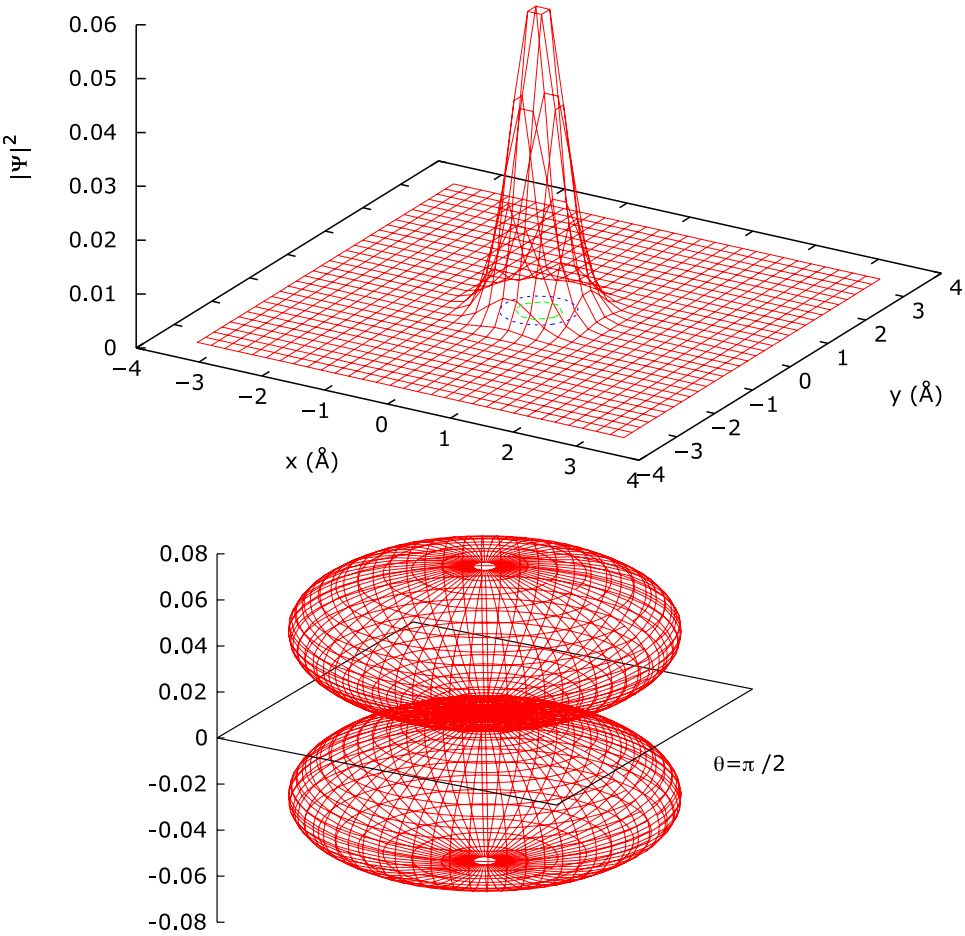

FIG. 4. Projection of the first excited state of the H_2@(8,0) system in the translational (upper panel) and rotational (lower panel) subspaces. The ϕ plane shown corresponds to a θ value of $\pi/2$.

nanotube: due to the tightness of the potential, all coordinates are even more coupled than they were in the wider (8,0) nanotube, which makes the study more difficult. The results of the qualitative analysis of the system are shown in Table IV. Note that, as predicted in the discussion about the potential energy surface, the energy pattern corresponds to that of a symmetric double-well system with a very high energy barrier: the eigenstates are numerically bidegenerate for all values of energy far below the top of the rotational barrier. This degeneracy is caused by a negligible tunnelling splitting. In the case of the ground state, the corresponding eigenfunctions are shown in Fig. 7, projected on the rotational degree of freedom. These functions appear localized around $\theta = 0$ and $\theta = \pi$, with an amplitude restricted to an arc of about 0.5 rad, which clearly means that this distortion is far too large for this coordinate to be inspected by direct comparison to rigid rotor functions. However, some quantum numbers have been assigned in the ϕ degree of freedom to represent the nodal planes which appear in this dimension. Concerning the other degrees of freedom, it should be pointed that the excitation energies are much larger in this case than in the previously studied, again due to the tighter potential. Note however that, in spite of the tightness of the potential, translational excited states in x and y degrees of freedom are still degenerate. As a final remark, in this system we do see vibrational excitations, which were too high in energy to be seen in the previous case and are now of the order of translational and rotational excitations.

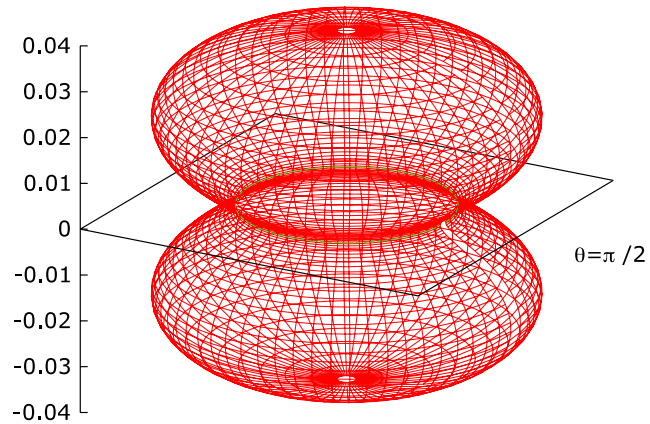

FIG. 5. Rotational projection of the total ground state wave function of H_2 in the (8,0) CNT. Note the significant depression for $\theta = \pi/2$.

B. Quantitative description of the eigenstates

It has been seen that a qualitative description of the eigenstates is not suitable for the H_2@SWCNT systems: even in the ground state, we find very significant deviations from the reference 2-D problem in the rotational degrees of freedom, and the translational functions also present variations between different energy levels which are not in a good agreement with a separable solution. Therefore, a quantitative analysis is desirable to truly obtain a meaningful correspondence between the eigenstates of the unbound and the confined molecule.

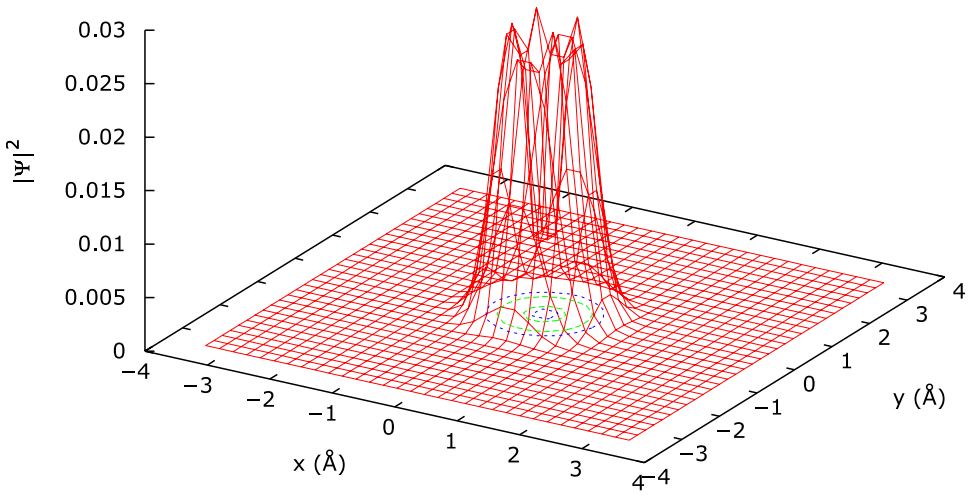

FIG. 6. Translational projection for the 11th excited state of the H_2@(8,0) system.

In order to perform this more rigorous analysis of the eigenfunctions of the system, a basis set is built from the solutions of an hypothetical separable Hamiltonian. This means that each element of the basis will be a direct product of functions corresponding to the different degrees of freedom of the system under study. For our specific problem, where the degrees of freedom are the internuclear distance, rotation, and translation of the center of mass of the molecule in the CNT potential, these basis functions have the form

$$\Phi^{k,l,m,n_x,n_y}(\rho,\theta,\phi,x,y) = M_k(\rho)Y_l^m(\theta,\phi)\Xi_{n_x,n_y}(x,y), \tag{8}$$

where each function of the product corresponds to the solution of a model system or to a eigenstate of a separable part of the Hamiltonian. Therefore, the functions which represent the internuclear distance, $M_k(\rho)$, and the rotation of the molecule, $Y_l^m(\theta,\phi)$, were built from the solution of two well-known problems, namely, the Morse potential and the rigid rotor, respectively. On the other hand, the translational functions, $\Xi_{n_x,n_y}(x,y)$, are chosen to be the solutions corresponding to a structureless particle moving in the xy plane, subjected to the potential created by the specific CNT under study, which resemble two-dimensional anharmonic oscillators.

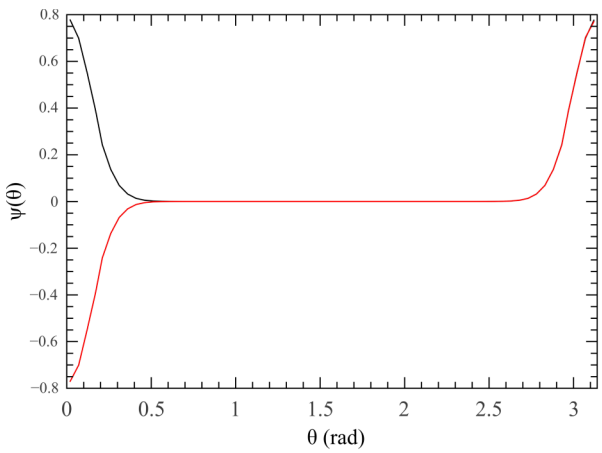

FIG. 7. Rotational projection of the degenerate ground state functions of the H_2@(5,0) system along the θ dimension, with $\phi = 0$.

The basis set is then built by adding each time a quantum to each degree of freedom. Once this is done, the actual system's eigenfunction can be represented in this basis

$$\Psi^n = \sum_{k=0}^{k_{max}} \sum_{l=0}^{l_{max}} \sum_{m=-l}^{l} \sum_{n_x=0}^{n_{x\,max}} \sum_{n_y=0}^{n_{y\,max}} c^n_{k,l,m,n_x,n_y} \Phi^{k,l,m,n_x,n_y}, \tag{9}$$

where the coefficients of the linear combination, c^n_{k,l,m,n_x,n_y}, can be obtained by performing the scalar product between a given function Ψ^n and each basis element

$$c^n_{k,l,m,n_x,n_y} = \langle \Psi^n \mid \Phi^{k,l,m,n_x,n_y} \rangle, \tag{10}$$

where m labels the basis element. These quantities give us a quantitative description of how much the actual eigenstate resembles that of the separable problem and therefore allows for a rigorous yet understandable interpretation of the quantum confinement phenomena.

The results for this analysis are given in Table V for the case of the $H_2(8,0)$ system. We can see that, except for the 1st excited state, all other eigenfunctions are not directly related to a single reference function, but rather with a linear combination of at least two of them. This agrees with the inconsistencies found during the interpretation of the wave function carried out in Sec. IV A: concerning the ground state, we see an important contribution of the $|02000\rangle$ function, which implies a contamination of the rotational subspace with the Y_2^0 function. Regarding the 11th excited state, whose projection we could not relate with any anharmonic oscillator function, its nature is also made clear by this analysis: the projection is just the result of a mixing of (0,1) and (1,0) states of the anharmonic oscillator. It should also be noted that, as the energy increases, the more reference functions are needed to represent accurately a given state.

For the case of the H_2@(5,0) system, the results of the full dimensional integration shown in Table VI differ significantly from those corresponding to the (8,0) nanotube: every state is a mixture of many more basis functions, even for the lowest energies. This means, as it was already pointed during the qualitative inspection of the mappings of the wave functions, that the distortions with respect to the free hydrogen case are much more important for the narrower nanotube.

TABLE V. Representation of the H_2@(8,0) system's eigenfunctions in the basis of direct product functions. Energies in cm^{-1} units. See Table ST1 in the supplementary material[19] for a complete table with all converged eigenstates.

State	ΔE	Basis element ($\|klmn_xn_y\rangle$)	$\|c^n_{k,l,m,n_x,n_y}\|$
0	0	$\|00000\rangle$	0.92
		$\|02000\rangle$	0.06
1	59	$\|01000\rangle$	0.98
2	171	$\|01100\rangle$	0.48
		$\|01-100\rangle$	0.48
3	171	$\|01100\rangle$	0.48
		$\|01-100\rangle$	0.48
4	265	$\|00001\rangle$	0.87
		$\|02001\rangle$	0.11
5	265	$\|00010\rangle$	0.85
		$\|00030\rangle$	0.02
		$\|02010\rangle$	0.10
6	310	$\|01001\rangle$	0.95
		$\|03001\rangle$	0.02
7	310	$\|01010\rangle$	0.92
		$\|01030\rangle$	0.04
8	343	$\|00000\rangle$	0.06
		$\|02000\rangle$	0.90
9	346	$\|02-100\rangle$	0.48
		$\|02100\rangle$	0.48
10	346	$\|02-100\rangle$	0.48
		$\|02100\rangle$	0.48
11	428	$\|01-101\rangle$	0.23
		$\|01-110\rangle$	0.25
		$\|01110\rangle$	0.25
		$\|01101\rangle$	0.23
12	429	$\|00010\rangle$	0.02
		$\|02-200\rangle$	0.48
		$\|02200\rangle$	0.48
13	429	$\|02200\rangle$	0.48
		$\|02-200\rangle$	0.48
14	462	$\|01110\rangle$	0.23
		$\|01101\rangle$	0.23
		$\|01-101\rangle$	0.23
		$\|01-110\rangle$	0.23
15	462	$\|01110\rangle$	0.23
		$\|01101\rangle$	0.23
		$\|01-101\rangle$	0.23
		$\|01-110\rangle$	0.23
16	503	$\|01110\rangle$	0.23
		$\|01101\rangle$	0.23
		$\|01-101\rangle$	0.23
		$\|01-110\rangle$	0.23
17	550	$\|00010\rangle$	0.74
		$\|02110\rangle$	0.16
18	550	$\|00002\rangle$	0.46
		$\|00020\rangle$	0.27
		$\|02002\rangle$	0.10
		$\|02020\rangle$	0.06
19	572	$\|00002\rangle$	0.30
		$\|00020\rangle$	0.44
		$\|02000\rangle$	0.03
		$\|02002\rangle$	0.06
		$\|02020\rangle$	0.08

TABLE VI. Representation of the H_2@(5,0) system's eigenfunctions in the basis of direct product functions. Energies in cm^{-1} units. See Table ST2 in the supplementary material[19] for a complete table with all converged eigenstates.

State	ΔE	Basis element ($\|klmn_xn_y\rangle$)	$\|c^n_{k,l,m,n_x,n_y}\|$
0	0	$\|00000\rangle$	0.072
		$\|02000\rangle$	0.282
		$\|12000\rangle$	0.032
		$\|32000\rangle$	0.018
		$\|04000\rangle$	0.096
		⋯	⋯
1	0	$\|01000\rangle$	0.199
		$\|03000\rangle$	0.309
		$\|11000\rangle$	0.029
		$\|13000\rangle$	0.030
		$\|31000\rangle$	0.023
		$\|33000\rangle$	0.020
		⋯	⋯
2	3552	$\|02-100\rangle$	0.017
		$\|02100\rangle$	0.065
		$\|12100\rangle$	0.012
		$\|04-100\rangle$	0.052
		$\|04100\rangle$	0.196
		$\|14100\rangle$	0.030
		$\|34100\rangle$	0.014
		⋯	⋯
3	3552	$\|02-100\rangle$	0.065
		$\|02100\rangle$	0.017
		$\|12-100\rangle$	0.012
		$\|04-100\rangle$	0.196
		$\|04100\rangle$	0.052
		$\|14-100\rangle$	0.030
		$\|34-100\rangle$	0.014
		⋯	⋯
4	3552	$\|01100\rangle$	0.016
		$\|03-100\rangle$	0.036
		$\|03100\rangle$	0.134
		$\|13100\rangle$	0.023
		⋯	⋯
5	3552	$\|01-100\rangle$	0.016
		$\|03-100\rangle$	0.134
		$\|03100\rangle$	0.035
		$\|13-100\rangle$	0.028
		⋯	⋯
6	3591	$\|00010\rangle$	0.067
		$\|02010\rangle$	0.264
		$\|03010\rangle$	0.013
		$\|12010\rangle$	0.031
		$\|32010\rangle$	0.017
		$\|04002\rangle$	0.091
		⋯	⋯
7	3591	$\|01010\rangle$	0.186
		$\|02010\rangle$	0.012
		$\|03010\rangle$	0.291
		$\|11010\rangle$	0.023
		$\|13010\rangle$	0.031
		$\|31010\rangle$	0.012
		$\|33010\rangle$	0.019
		⋯	⋯

Table VI shows an important feature of the system: note that for some states, basis functions with both even and odd quantum numbers, l, have a relevant contribution in the final state. This feature is a result of the exceptionally large rotational barrier of the confined hydrogen molecule. This hindrance in the angular degree of freedom, as it was discussed earlier, forces a numerical bidegeneracy of the rotational energy levels of the hydrogen molecule. If symmetry conditions are not imposed for the eigenstates of the system, two possible solutions are equally valid: a delocalized representation of the wave function or a localized representation made from the linear combination of symmetric and antisymmetric states. In our case, the basis set employed is formed of functions without any parity, which favours (but does not force) the localized representation of the eigenstates. Finally, another important difference between the hydrogen molecules confined in the (8,0) or the (5,0) nanotube is found in the ρ degree of freedom: for the narrower CNT, vibrationally excited states contribute to the wave function already in the 3rd excited state, while no excitations were found during the analysis of the H_2@(8,0) system's eigenstates.

The full dimensional overlap offers a direct and simple view of the total wave function as a combination of well-known reference states. Yet, it is still difficult to get an insight into the dynamics of the confined hydrogen molecule just by observing these quantities, since the actual wave function, which gives information about the probability of finding the molecule in a given position and orientation, is lost when performing the scalar products. Our aim here is to develop a representation of the wave function which allows an intuitive understanding of the motion of H_2 inside a confining structure, while maintaining a rigorous approach.

Following this idea, we computed a partial overlap function, $\sigma(\vec{x}_{red})$, between the full five-dimensional wave function corresponding to each eigenstate and a model function corresponding to a *logical* coordinates of the system. These *logical* coordinates are understood as strongly coupled degrees of freedom which cannot be straightforwardly separable. In our case, these will be rotation on one hand and translation of the center of mass on the other. Hence, the magnitudes that we will study will be

$$\sigma_{l,m}(\rho,x,y) = \langle \psi(\rho,\theta,\phi,x,y) \mid Y_l^m(\theta,\phi)\rangle = \int_0^{2\pi}\int_0^{\pi} \psi(\rho,\theta,\phi,x,y)^*\, Y_l^m(\theta,\phi)\, sin\theta\, d\theta\, d\phi, \tag{11}$$

$$\sigma_{n_x,n_y}(\rho,\theta,\phi) = \langle \psi(\rho,\theta,\phi,x,y) \mid \Xi_{n_x,n_y}(x,y)\rangle = \int_{-\infty}^{\infty}\int_{-\infty}^{\infty} \psi(\rho,\theta,\phi,x,y)^*\, \Xi_{n_x,n_y}(x,y)\, dx\, dy, \tag{12}$$

where the model functions for the rotational degrees of freedom are the same that were used for the definition of the full dimensional overlap. We will refer to these quantities as rotational and translational overlap functions, respectively.

Note that the magnitudes in Eqs. (11) and (12) are scalar products between functions of different dimensionalities. Hence, there are three features that must be taken into account for their correct interpretation:

1. Since we are integrating the functions in a 2-D subspace of the 5-D total space, this product is a function of the three non-integrated degrees of freedom. This will allow us to see how the states corresponding to the reference problem change their contribution as the potential changes.
2. Both the total 5-D function and the reference 2-D ones are normalized in the space they span, and for that the scalar product will *not* be normalized, but rather depend on the norm of the total 5-D function in each point of the non-integrated space. This will allow us to focus on the region in which the total wave function is relevant.
3. For each point of the full 5-D space, the total wave function can be obtained through a direct product of the sum of partial overlaps for the different degrees of freedom. For a system divided in q logical coordinates, each containing k_q degrees of freedom

$$\Psi^n(\vec{\mathbf{x}}) = \prod_q \left(\sum_{j_1} \cdots \sum_{j_{k_q}} \sigma_q(\vec{x}_q) \right). \tag{13}$$

In our specific case,

$$\Psi^n(\vec{\mathbf{x}}) = \left(\sum_k \sigma_k(\theta,\phi,x,y) M_k(\rho) \right) \times \left(\sum_l \sum_m \sigma_{l,m}(\rho,x,y) Y_l^m(\theta,\phi) \right) \times \left(\sum_{n_x} \sum_{n_y} \sigma_{n_x,n_y}(\rho,\theta,\phi) \Xi_{n_x,n_y}(\theta,\phi) \right). \tag{14}$$

In short, from the study of the overlap function in the different subspaces, we obtain quantitative information of both the norm of the total wave function in a given point and about its shape, through the interpretation of the overlap as the coefficients of the linear combination of basis functions, which gives rise to the eigenstate. Then, the study of these functions allows a straightforward interpretation of the dynamics of the hydrogen molecule, since we can see directly how the coupling between different degrees of freedom affects the dynamics.

Still, the analysis of a three-dimensional object is not a trivial task; it is always easier to study the trends of one-dimensional functions. To further reduce the dimensionality of the problem, we take advantage of two characteristic features of the system: first, no vibrational excitations are observed within the first 50 calculated eigenstates. This feature will allow us to explore the behaviour of $\sigma_{n_x,n_y}(\rho,\theta,\phi)$ and $\sigma_{l,m}(\rho,x,y)$ for a fixed $\rho = 1.41$ bohrs, which corresponds to the internuclear distance with maximum probability density for the vibrational ground state. The second feature is the symmetry of the eigenfunctions studied: in the translational subspace, they are all either cylindrical or mainly located along two orthogonal axes, which we can consider as the x and y axes. Therefore, we can focus on the values of the functions along these axes. On the other hand, the rotational functions can be scanned along the range of θ from 0 to π for, in principle, any value of ϕ. However, in spite of the isotropy of the potential for the (8,0) nanotube, the rotational eigenfunctions will not be isotropic and may present several nodal planes in both θ or ϕ coordinates. Therefore, we do not have a preferred value of the coordinates to scan *a priori*, since any arbitrary value

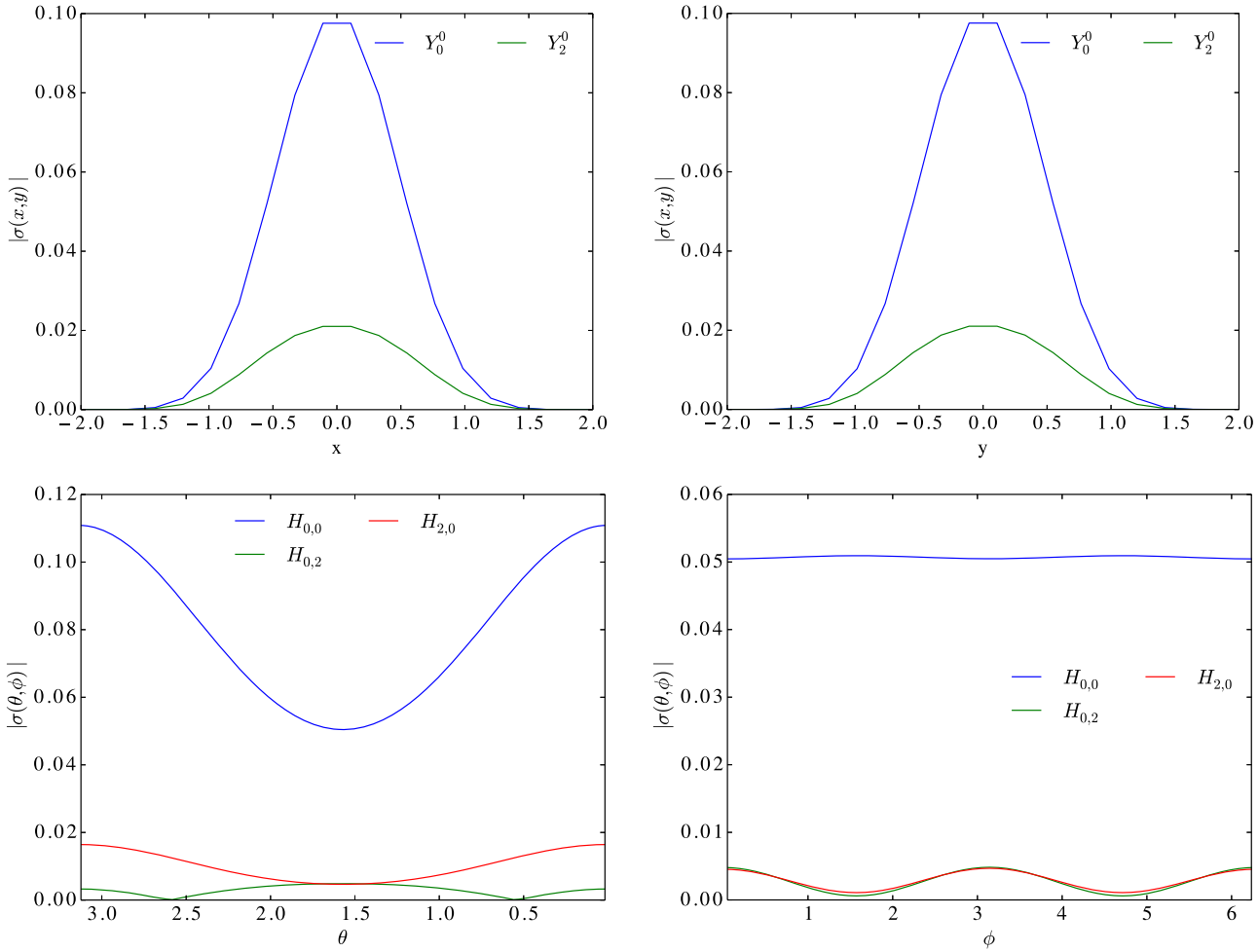

FIG. 8. Analysis of the ground state eigenfunction of the H_2@(8,0) system. Upper panel: Radial overlap function along the x and y axes for the ground state function. Lower panel: Translational overlap function along θ for $\phi = 0$ and along ϕ for $\theta = \pi/2$.

of the angle may in principle correspond to a nodal plane for some eigenstate of the system. The pair of angles which will be scanned therefore will depend on the particular function under study. A general rule could be that the fixed value of ϕ along which the θ dimension will be scanned may correspond to the point in which the translational overlap function, $\sigma_{n_x,n_y}(\rho,\theta,\phi)$, presents a maximum. The same can be used to select the fixed value of θ for which ϕ will be studied. Yet, this

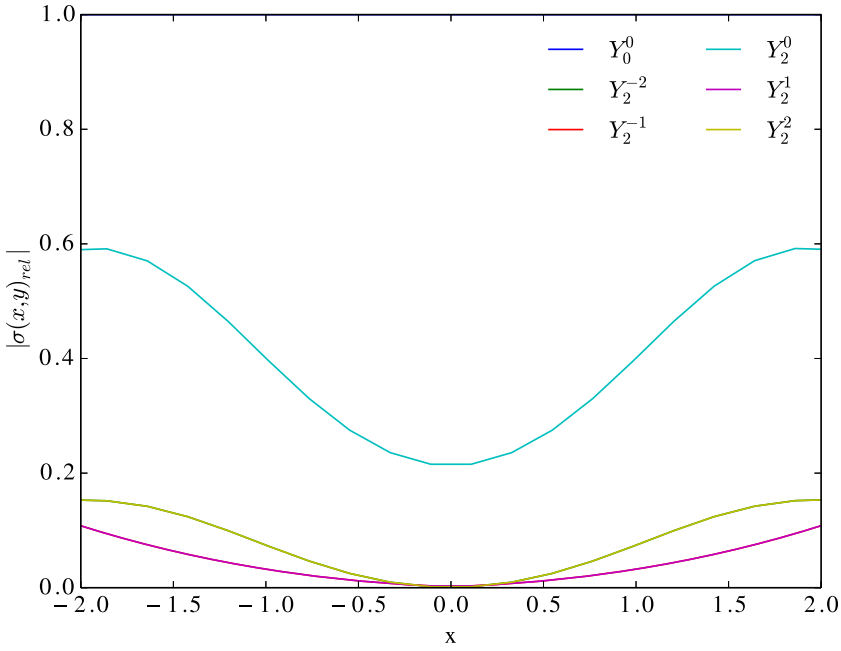

FIG. 9. Representation of the most relevant relative rotational overlap functions for the ground state in the H_2@(8,0) system.

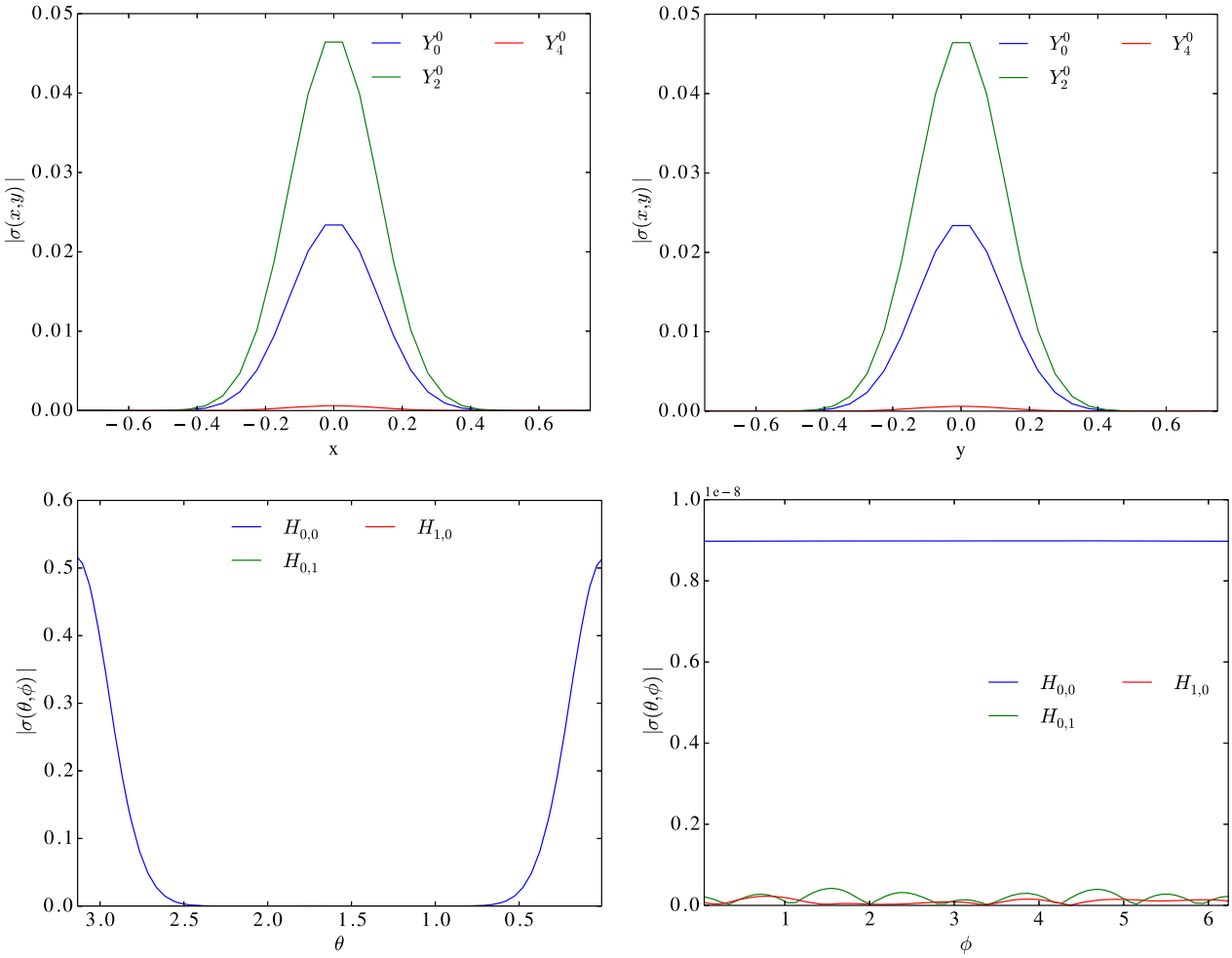

FIG. 10. Upper panel: Radial overlap function along the x and y axes for the ground state wave function in the H_2@(5,0) system. Lower panel: Translational overlap function along θ for $\phi = 0$ and along ϕ for $\theta = 0$.

criterion may be altered in favour of a more physically relevant pair.

It shall be noted that this reduction of the dimensionality is carried out only with the aim of easing the interpretation and gives a general overview of the H_2@SWCNT systems under study. The overlap functions in the different subspaces are obtained without calling on any approximation and therefore can be used to study any wave function in an arbitrary point of the space in a rigorous way.

Starting with the H_2@(8,0) system, we have obtained the three-dimensional overlaps with the rotational (Eq. (11)) and translational (Eq. (12)) model functions. As an example, in Figure 8, the absolute values of the rotational and translational overlap functions for the ground state with the most relevant test functions are shown along the four directions outlined previously (θ, ϕ, x and y). Each line in the plot corresponds to the overlap function related to a single reference state. It is readily seen that this state does not correlate with a single state of the free H_2 molecule, but it rather has many contributions. These contributions, as it was predicted, vary significantly depending on the orientation and position of the c.o.m of the H_2 molecule, thus confirming the strong coupling between the translational and internal degrees of freedom in all the eigenstates of the system. In particular, it can be seen how, although the major contribution to the ground state comes from the Y_0^0 and $H_{0,0}$ states, there is a significant contribution of the Y_2^0 state in all the translational subspace. Similarly, we see an important contribution of the $H_{2,0}$ and $H_{0,2}$ states, which hits a maximum proportion in the region near $\theta = 0$.

Therefore, these plots allow us to determine the shape of the eigenstate at a given point. Furthermore, since the overlap function is *weighted* by the total norm of the wave function in a given point, non-relevant areas in the total sampling space simply do not appear, which is a great advantage. However, this feature introduces a problem in the interpretation for the translational degrees of freedom: since the probability density in these coordinates has a gaussian-like shape, it decreases rapidly when the molecule gets closer to the nanotube's walls. This makes it difficult to see how the relative contribution of the model states changes away from the center of the nanotube, which is the key to see if the system becomes more distorted as we approach the nanotube's wall. To overcome this difficulty, we plot the *relative* overlap function in the translational space, which results from dividing the rotational overlap for each reference function with the rotational overlap function of the dominant state, i.e., the state which has the maximum contribution to the total wave function, denoted $\sigma_{l^{dom},m^{dom}}$,

$$\sigma^{rel}_{l,m}(\rho,x,y) = \frac{\sigma_{l,m}}{\sigma_{l^{dom},m^{dom}}}, \tag{15}$$

TABLE VII. Results of the quantitative description of the eigenstates of the H_2@(8,0) system. Energies referred to the ground state energy of 2580 cm^{-1}, contribution of the reference functions referred to the point of maximum probability density in the 5D space. See Table ST3 in the supplementary material[19] for a complete table with all converged eigenstates.

							Model functions contribution			
State	ΔE	ρ	θ	ϕ	x	y	l,m	$\lvert\sigma^n_{l,m}\rvert$	n_x,n_y	$\lvert\sigma^n_{n_x,n_y}\rvert$
0	0	1.4	0.0	0.0	0.0	0.0	(0, 0)	0.097	(0, 0)	0.11
							(2, 0)	0.021	(0, 2)	0.02
1	59	1.4	π	0.0	0.0	0.0	(1, 0)	0.096	(0, 0)	0.14
							...	...	(0, 2)	0.02
2	171	1.4	1.8	$\pi/2$	0.0	0.0	(1, 1)	0.011	(0, 0)	0.11
							(1, −1)	0.011	...	...
3	171	1.4	1.25	π	0.0	0.0	(1, 1)	0.073	(0, 0)	0.11
							(1, −1)	0.073	(2, 0)	0.01
							...	...	(0, 2)	0.01
4	265	1.4	π	$\pi/4$	0.55	0.0	(0, 0)	0.084	(0, 1)	0.12
							(2, 0)	0.028	(1, 2)	0.02
5	265	1.4	π	$3\pi/4$	0.0	0.55	(0, 0)	0.084	(1, 0)	0.12
							(2, 0)	0.028	(0, 3)	0.03
6	310	1.4	π	1.32	0.55	0.0	(1, 0)	0.087	(0, 1)	0.15
							...	...	(1, 2)	0.02
7	310	1.4	π	2.90	0.0	0.55	(1, 0)	0.087	(1, 0)	0.15
							...	...	(0, 3)	0.04
8	343	1.4	π	0.0	0.0	0.0	(0, 0)	0.038	(0, 0)	0.15
							(2, 0)	0.092	(0, 2)	0.03
							...	...	(2, 0)	0.01
9	346	1.4	$3\pi/4$	$\pi/2$	0.0	0.0	(2, 1)	0.070	(0, 0)	0.14
							(2, −1)	0.070	(0, 1)	0.01
10	346	1.4	$3\pi/4$	π	0.0	0.0	(2, 1)	0.070	(0, 0)	0.14
							(2, −1)	0.070	(0, 2)	0.02
11	428	1.4	1.1	$\pi/2$	0.33	0.33	(1, −1)	0.048	(1, 0)	0.08
							(1, 1)	0.048	...	...
12	429	1.4	$\pi/2$	$\pi/4$	0.0	0.0	(2, 2)	0.011	(0, 0)	0.13
							(2, −2)	0.011	(1, 1)	0.01
							...	...	(2, 0)	0.01
							...	...	(0, 2)	0.01
13	429	1.4	$\pi/2$	$\pi/2$	0.0	0.0	(2, 2)	0.073	(0, 0)	0.13
							(2, −2)	0.073	...	...
14	462	1.4	2.18	4.76	0.32	0.32	(1, 1)	0.050	(1, 0)	0.07
							(1, −1)	0.050	...	...
15	462	1.4	2.09	1.62	0.0	0.55	(1, 1)	0.048	(0, 1)	0.08
							(1, −1)	0.048	...	...
16	503	1.4	h.0	0.0	0.0	0.0	(1, 1)	0.050	(1, 0)	0.08
							(1, −1)	0.050	(0, 3)	0.01
17	550	1.4	π	$\pi/4$	0.55	0.55	(0, 0)	0.067	(1, 1)	0.13
							(2, 0)	0.031	...	...
18	550	1.4	π	0.54	−0.76	0.0	(0, 0)	0.067	(0, 0)	0.01
							(2, 0)	0.031	(2, 0)	0.11
							...	...	(0, 2)	0.08
19	572	1.4	0.0	3.0	0.0	0.0	(0, 0)	0.085	(0, 0)	0.03
							(2, 0)	0.051	(2, 0)	0.08
							...	...	(0, 2)	0.10
20	580	1.4	3.0	$\pi/4$	−0.55	0.55	(1, 0)	0.075	(1, 1)	0.15
							(3, 0)	0.014	...	...

always considering only the space in which the total wave function has a relevant value, in order to have a well-behaved function.

The plot of the relative overlap functions corresponding to the upper left panel of Figure 8, corresponding to the rotational overlap function along the x coordinate for the ground state of the H_2@(8,0) system, is shown in Figure 9. It is readily seen that the percentage of contribution of high-energy reference states increases as we get close to the nanotube's walls, changing from a mixture of Y_0^0/Y_2^2 in a 5/1 proportion in the center of the nanotube to a mixture of 5 states, where the main one has less than a 50% of contribution. This fact illustrates the effects of the coupling on the overall function.

The general trends observed in the study are that the higher the energy of the studied state, the more eigenstates of the free molecule contribute to it, even though in general there is always a dominant contribution to a given state. This is consistent with the fact that in excited eigenstates, the maximum probability density is located in areas where the potential affects more strongly, thus further increasing the distortion with respect to the reference functions. Therefore, it is clear that the coupling between the different degrees of freedom forces us to study the whole subspaces in which the overlap function is represented in order to understand the system.

The quantitative study of the eigenstates of the H_2 molecule in the narrower (5,0) nanotube confirms what was expected from all the previous studies (qualitative analysis of both the PES and the projected eigenfunctions, as well as the full-dimensional overlap study): a tighter potential increases the couplings in the system, and therefore, the distortions away from the model states are even more noticeable. However, the partial overlap functions allow us to find how the different degrees of freedom are distorted. As seen in Figure 10, for the ground state of the system, the translational part of the wave function does not differ much from the structureless particle in the anharmonic potential. This apparent small coupling between the internal and translational degrees of freedom, which is surprising at first glance, can be understood in terms of the hindered rotation: for this system, the hydrogen molecule is forced to remain almost parallel to the nanotube's axis, which is the disposition that is more similar in energy to a structureless particle, in terms of the potential energy surface. Therefore, there is indeed a strong coupling between the degrees of freedom, but it is not seen as a mixing of states, but rather as a localization of the wave function.

To obtain precise information of relevant points of the whole 5D space spanned by the systems under study, we can take advantage of Eq. (14), which expresses the wave function in a given point as a direct product of the linear combination of the different basis functions, with the coefficient of the combinations being the value of the overlap function in that point. This interpretation allows an intuitive understanding of the high dimensional wave function in a single point of the space in terms of the more familiar one or two dimensional model functions.

In Tables VII and VIII, the lowest energy states are shown for the H_2@(8,0) and H_2@(5,0), respectively, following this idea: for each function, the point in the 5D space with the highest probability density is selected. Then, for this point, the model functions which contribute the most to the system are listed together with the absolute value of their coefficient in the linear combination (i.e., the value of the corresponding overlap function). Note that, for the sake of clarity, the absolute value of the coefficient is given instead of the complex number, and therefore, the phase of the combination is disregarded.

Table VII offers a summary of the information obtained for the H_2@(8,0) system. It can be seen that the results are in general consistent with the overlap with 5D basis functions and the overlap functions plots. However, we must take into account a conceptual difference between these two analyses: the full overlap carried out previously gave us information about the averaged wave function in all the spanned space, whereas these overlap functions focus on different points in a given

TABLE VIII. Results of the quantitative description of the eigenstates of the H_2@(5,0) system. Energies referred to the ground state energy of 9273 cm^{-1}, contribution of the reference functions referred to the point of maximum probability density in the 5D space. See the supplementary material[19] (Table ST4) for a complete table with all converged eigenstates.

							Model functions contribution			
State	ΔE	ρ	θ	ϕ	x	y	l,m	$\lvert\sigma^n_{l,m}\rvert$	n_x,n_y	$\lvert\sigma^n_{n_x,n_y}\rvert$
0	0	1.3	π	0	0.025	0.025	(0,0)	0.023	(0,0)	0.52
							(2,0)	0.046	…	…
							(4,0)	0.027	…	…
1	0	1.3	0.0	5.7466	−0.025	−0.025	(1,0)	0.039	(0,0)	0.51
							(3,0)	0.049	…	…
2	3552	1.3	0.22	$\pi/4$	−0.025	−0.025	(2,−1)	0.011	(0,0)	0.41
							(2,1)	0.022	(2,0)	0.06
							(4,−1)	0.020	…	…
							(4,1)	0.039	…	…
3	3552	1.3	0.22	π	0.025	0.025	(2,−1)	0.022	(0,0)	0.41
							(2,1)	0.011	(0,1)	0.06
							(4,−1)	0.039	…	…
							(4,1)	0.020	…	…
4	3552	1.3	2.91	$\pi/4$	−0.025	0.025	(1,−1)	0.006	(0,0)	0.41
							(1,1)	0.011	(2,0)	0.06
							(3,−1)	0.016	…	…
							(3,1)	0.032	…	…
5	3552	1.3	2.91	2π	0.025	−0.025	(1,−1)	0.011	(0,0)	0.41
							(1,1)	0.006	(2,0)	0.06
							(3,−1)	0.032	…	…
							(3,1)	0.016	…	…

subspace. The different natures of the analysis can lead to some inconsistencies. For instance, the translational contributions in 11th excited state indicate that only the $n_x = 1, n_y = 0$ function contributes to that point. This apparent inconsistency arises due to the cylindrical symmetry of this state in the xy subspace, since we have selected just a point as representative of a whole set of points which present the same density.

Table VIII summarizes an overview of the main contributions to the different wave functions calculated for the H_2@(5,0) system. Oppositely from what was found for the previous system, in which most states where a combination of two or three functions of the model systems at most, what is found here is that the wave function has many more contributions. We refer to the supplementary material[19] Table ST2 for information about higher energy states. Note that in this case, the values of maximum probability on the internuclear distance change on some states, due to the presence of excited states in this DoF.

V. SUMMARY AND CONCLUSIONS

A novel view in the study of nuclear eigenstates of systems with important couplings between different degrees of freedom has been developed through the computation and analysis of different overlap functions rather than of the reduced probability density. This method allows to get an insight into how the system behaves in the different points of the space under study. Our approach has been applied to two nanoconfined systems, being the first a technologically relevant system in which confinement effects have been previously studied (a single hydrogen molecule confined in an (8,0) carbon nanotube) and the second an academic case in which the confining potential is still more hindering (the H_2@(5,0) system). In both cases, the results extracted of a qualitative inspection of the reduced probability density of the system were compared with the results of our quantitative study made through overlap functions.

The analysis shows clearly that the qualitative inspection of reduced density functions can lead to erroneous interpretations, because the non-separability of the Hamiltonian prevents the assignation of the usual quantum numbers to the different degrees of freedom. The study of the overlap functions in suitable subspaces, on the other hand, offers an intuitive and rigorous image of the dynamics of the embedded molecule, allowing to see the changes of the wave function in the different points of the space.

ACKNOWLEDGMENTS

We acknowledge financial support from the Spanish Ministerio de Economa y Competitividad (Ministry of Economy and Competitiveness) (CTQ2013-41307-P) and Generalitat de Catalunya (2014-SGR-25). M.M.-M. further thanks a predoctoral grant from the FPU program (FPU2013/02210) of the Spanish Ministerio de Educacin, Cultura y Deporte (Ministry of Education, Culture and Sports, Spain). We also thank Dr. Jaime Suárez for useful discussions.

[1]M. Xu, L. Ulivi, M. Celli, D. Colognesi, and Z. Bačić, "Rigorous quantum treatment of inelastic neutron scattering spectra of a heteronuclear diatomic molecule in a nanocavity: HD in the small cage of structure II clathrate hydrate," Chem. Phys. Lett. **563**, 1–8 (2013).
[2]T. Rõõm, L. Peedu, M. Ge, D. Hüvonen, U. Nagel, S. Ye, M. Xu, Z. Bačić, S. Mamone, M. H. Levitt, M. Carravetta, J. Y.-C. Chen, X. Lei, N. J. Turro, Y. Murata, and K. Komatsu, "Infrared spectroscopy of small-molecule endofullerenes," Philos. Trans. Ser. A: Math., Phys. Eng. Sci. **371**, 20110631 (2013).
[3]Q. Wang, S. Challa, D. Sholl, and J. Johnson, "Quantum sieving in carbon nanotubes and zeolites," Phys. Rev. Lett. **82**, 956–959 (1999).
[4]S. Fatemi, M. Vesali-Naseh, M. Cyrus, and J. Hashemi, "Improving CO_2/CH_4 adsorptive selectivity of carbon nanotubes by functionalization with nitrogen-containing groups," Chem. Eng. Res. Des. **89**, 1669–1675 (2011).
[5]T. Lu, E. Goldfield, and S. Gray, "Quantum states of hydrogen and its isotopes confined in single-walled carbon nanotubes: Dependence on interaction potential and extreme two-dimensional confinement," J. Phys. Chem. B **110**, 1742–1751 (2006).
[6]T. Yildirim and A. Harris, "Quantum dynamics of a hydrogen molecule confined in a cylindrical potential," Phys. Rev. B **67**, 245413 (2003).
[7]I. Matanović, J. L. Belof, B. Space, K. Sillar, J. Sauer, J. Eckert, and Z. Bačić, "Hydrogen adsorbed in a metal organic framework-5: Coupled translation-rotation eigenstates from quantum five-dimensional calculations," J. Chem. Phys. **137**, 014701 (2012).
[8]S. Ye, M. Xu, S. FitzGerald, K. Tchernyshyov, and Z. Bacic, "H_2 in solid C_{60}: Coupled translation-rotation eigenstates in the octahedral interstitial site from quantum five-dimensional calculations," J. Chem. Phys. **138**, 244707 (2013).
[9]T. K. Nielsen, U. Bösenberg, R. Gosalawit, M. Dornheim, Y. Cerenius, F. Besenbacher, and T. R. Jensen, "A reversible nanoconfined chemical reaction," ACS Nano **4**, 3903–3908 (2010).
[10]C. I. Contescu, H. Zhang, R. J. Olsen, E. Mamontov, J. R. Morris, and N. C. Gallego, "Isotope effect on adsorbed quantum phases: Diffusion of H_2 and D_2 in nanoporous carbon," Phys. Rev. Lett. **110**, 236102 (2013).
[11]S. FitzGerald, T. Yildirim, L. Santodonato, D. Neumann, J. Copley, J. Rush, and F. Trouw, "Quantum dynamics of interstitial H2 in solid C60," Phys. Rev. B **60**, 6439–6451 (1999).
[12]T. Yildirim and A. Harris, "Rotational and vibrational dynamics of interstitial molecular hydrogen," Phys. Rev. B **66**, 214301 (2002).
[13]J. Suarez and F. Huarte-Larrañaga, "Hydrogen confined in single-wall carbon nanotubes: Anisotropy effects on ro-vibrational quantum levels," J. Chem. Phys. **137**, 064320 (2012).
[14]R. Dovesi, R. Orlando, B. Civalleri, C. Roetti, V. R. Saunders, and C. M. Zicovich-Wilson, "CRYSTAL: A computational tool for the *ab initio* study of the electronic properties of crystals," Z. Kristallogr. **220**, 571–573 (2005).
[15]R. Dovesi, V. R. Saunders, C. Roetti, R. Orlando, C. M. Zicovich-Wilson, F. Pascale, B. Civalleri, K. Doll, N. M. Harrison, I. J. Bush, P. D'Arco, and M. Llunell, *CRYSTAL09 User's Manual* (University of Torino, Torino, 2009).
[16]P. Morse, "Diatomic molecules according to the wave mechanics. II. Vibrational levels," Phys. Rev. **34**, 57–64 (1929).
[17]A. Novaco and J. Wroblewski, "Rotational states of H_2, HD, and D_2 on graphite," Phys. Rev. B **39**, 11364–11371 (1989).
[18]F. Huarte-Larrañaga and M. Albertí, "A molecular dynamics study of the distribution of molecular hydrogen physisorbed on single walled carbon nanotubes," Chem. Phys. Lett. **445**, 227–232 (2007).
[19]See supplementary material at http://dx.doi.org/10.1063/1.4913293 for complete tables and additional figures.
[20]U. Manthe, "The state averaged multiconfigurational time-dependent Hartree approach: Vibrational state and reaction rate calculations," J. Chem. Phys. **128**, 064108 (2008).
[21]H.-D. Meyer, U. Manthe, and L. Cederbaum, "The multi-configurational time-dependent Hartree approach," Chem. Phys. Lett. **165**, 73–78 (1990).
[22]*Multidimensional Quantum Dynamics*, edited by H.-D. Meyer, F. Gatti, and G. A. Worth (Wiley-VCH Verlag GmbH & Co. KGaA, Weinheim, Germany, 2009).
[23]H.-D. Meyer, F. Gatti, and G. A. Worth, "Kinetic energy operators," in *Multidimensional Quantum Dynamics*, edited by H.-D. Meyer, F. Gatti, and G. A. Worth (Wiley-VCH Verlag GmbH & Co. KGaA, 2009), pp. 91–110.
[24]"Correlation discrete variable representation (CDVR)," *Multidimensional Quantum Dynamics. MCTDH Theory and Applications*, edited by H.-D. Meyer, F. Gatti, and G. A. Worth (Wiley-VCH Verlag GmbH & Co. KGaA, 2009), pp. 73–80.
[25]J. Schiff and B. Poirier, "Communication: Quantum mechanics without wavefunctions," J. Chem. Phys. **136**, 031102 (2012).